In the foregoing discussion, we ignore the possibility of a worldwide cyclicity in the process of continental accretion (*25*). Demonstration of undoubted cyclicity of this kind would logically force refinement of estimates of our mass transfer rates for the past to fit some cyclic pattern. We note also that a detailed consideration of the geochemical evolution of the mantle may ultimately suggest other refinements in our model. The most obvious implication of the model in this context is the inference that the composition of the present lithosphere is a key to the composition of the inner mantle. A second logical consequence of the proposed model is that the material of the asthenosphere, rather than the mesosphere, most closely approximates a primitive composition.

Our hypothesis of sinking lithosphere, accretionary mesosphere, and shrinking asthenosphere is a dynamic model for the irreversible evolution of the entire mantle at a rate linked to the rate of production of radiogenic heat in the earth. Appropriate assumptions produce a viable semiquantitative model in terms of the mass transfer required within the time available and also are in reasonable accord with corollary inferences about the growth of continents. No physicochemical details have been treated, as our intent has been to test the overall model to a first approximation. Simple extrapolation of the assumptions we have made for the past into the future indicates that an earth lacking asthenosphere and presumably incapable of plate tectonic behavior as we now know it will be produced in less than 10^9 years. It is conceivable to us that apparently "dead" planetary bodies, like the moon and Mars, may have reached such a state by completing an internal evolution similar to the one that we suggest is now in progress in the earth's mantle.

W. R. DICKINSON
W. C. LUTH

Geology Department,
Stanford University,
Stanford, California 94305

References and Notes

1. B. Isacks, J. Oliver, L. R. Sykes, *J. Geophys. Res.* **73**, 5855 (1968).
2. J. Oliver, *Phys. Earth Planet. Inter.* **2**, 350 (1970).
3. B. Isacks and P. Molnar, *Nature* **223**, 1121 (1969).
3a. W. M. Elsasser, *J. Geophys. Res.* **76**, 4744 (1971).
4. H. Kanamori and F. Press, *Nature* **226**, 330 (1970).
5. D. L. Anderson, *Science* **157**, 1165 (1967).
6. A. E. Ringwood, in *The Earth's Crust and Upper Mantle*, P. J. Hart, Ed. (American Geophysical Union Monograph No. 13, Washington, D.C., 1969), p. 1.
7. J. R. Heirtzler, G. O. Dickson, E. M. Herron, W. C. Pitman III, X. LePichon, *J. Geophys. Res.* **73**, 2119 (1968).
8. F. J. Vine, *J. Geol. Educ.* **18**, 87 (1970).
9. W. M. Elsasser, *J. Geophys. Res.* **76**, 1101 (1971).
10. F. J. Vine, *J. Geol. Educ.* **17**, 6 (1969).
11. J. Oliver and B. Isacks, *J. Geophys. Res.* **72**, 4259 (1967).
12. D. L. Anderson, C. Sammis, T. Jordan, *Science* **171**, 1103 (1971).
13. A. E. Lubimova, in *The Earth's Crust and Upper Mantle*, P. J. Hart, Ed. (American Geophysical Union Monograph No. 13, Washington, D.C., 1969), p. 63.
14. F. Birch, *J. Geophys. Res.* **69**, 4377 (1964); *Bull. Geol. Soc. Amer.* **76**, 133 (1965).
15. J. F. Lovering and J. W. Morgan, *J. Geophys. Res.* **69**, 1979 (1964).
16. G. J. Wasserburg, G. J. F. MacDonald, F. Hoyle, W. A. Fowler, *Science* **143**, 465 (1964).
17. F. Press, *ibid.* **160**, 1218 (1968).
18. W. R. Dickinson, *Rev. Geophys. Space Phys.* **8**, 813 (1970); E. L. Oxburgh and D. L. Turcotte, *Bull. Geol. Soc. Amer.* **81**, 1665 (1970); *J. Geophys. Res.* **76**, 1315 (1971).
19. D. E. Karig, *J. Geophys. Res.* **76**, 2542 (1971).
20. R. L. Armstrong, *Rev. Geophys.* **6**, 175 (1968).
21. S. R. Taylor, *Tectonophysics* **4**, 17 (1967).
22. P. M. Hurley and J. R. Rand, *Science* **164**, 1229 (1969).
23. P. M. Hurley, H. Hughes, G. Faure, H. W. Fairbairn, W. H. Pinson, *J. Geophys. Res.* **67**, 5315 (1962); A. E. J. Engel, *Science* **140**, 143 (1963).
24. P. B. King, *U.S. Geol. Surv. Prof. Pap. 628* (1969), p. 1.
25. J. Sutton, *Nature* **198**, 731 (1963).
26. Supported in part by NSF grant G1684.

21 July 1971

Hyperfine Zeeman Effect
Atomic Absorption Spectrometer for Mercury

Abstract. *A new type of atomic absorption spectrometer—one that detects trace mercury in host material, based on hyperfine structure lines in a magnetic field—was developed and tested on various substances. This device can detect trace mercury to about 0.04 part per million (40 parts per billion) in about 1 minute. No chemical separation from the host material is necessary.*

A problem of importance today is the detection of mercury in food, especially in fish such as tuna and swordfish. Unfortunately, as far as we know, no device available yields a rapid determination of mercury to about 0.1 ppm in about 1 minute without preliminary separation of the mercury from the host material. Because of the urgent need for the detection of mercury, we have converted to this purpose a mercury optical-pumping nuclear magnetic resonance magnetometer (*1*) which we had contructed to measure magnetic fields. We were motivated to use this technique because we can observe routinely in our magnetometer a magnetic resonance signal whose equivalent density is about 10^{10} to 10^{11} atoms per cubic centimeter. This corresponds to about 10^{-12} g of mercury per cubic centimeter. Because of the intrinsic power of detection of this apparatus and because considerable work had been done to construct a stable, intense, sharp mercury lamp and associated electronic equipment, we believed that converting the magnetometer to a mercury detector would be useful.

Our objective was to develop an instrument that can be operated by completely inexperienced personnel (such as fishermen), has high accuracy in mercury detection to at least 0.04 ppm (40 ppb), is very rapid in analysis without any chemical separation from the host material, and is inexpensive. We believe that our prototype instrument satisfies the above aims, although the unit in its present form is not quite

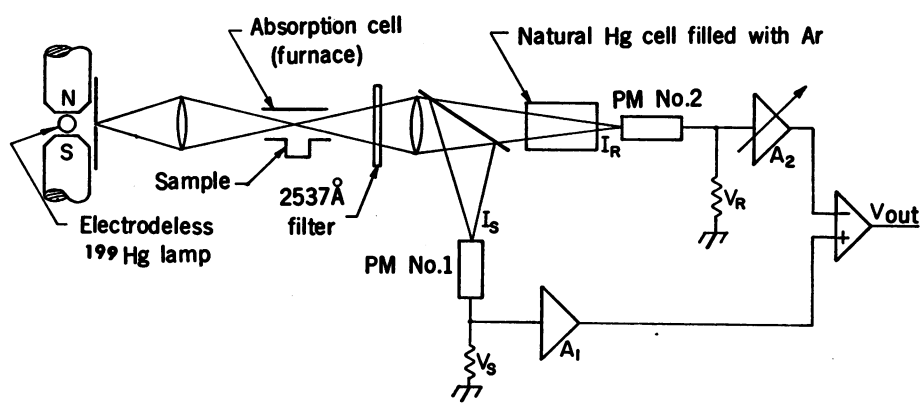

Fig. 1. Block diagram illustrating the principle of operation of the device.

portable because we used readily available materials instead of engineering a commercial-type unit.

In illustrating the principle of operation of this device, we describe first an ideal case and then an alternative way to approach this ideal condition, which is more difficult to achieve in practice. Let us consider an even-isotope mercury lamp placed in a high magnetic field (about 20 to 30 kgauss). The resonance radiation at a wavelength (λ) of 2537 Å, corresponding to $^3P_1 \rightarrow {}^1S_0$ transitions, is split into three components: σ^+, π, and σ^-. The light emitted in the direction normal to the magnetic field consists of three Zeeman components whose frequencies ν are given by

$$\begin{aligned} \nu(\sigma^+) &= \nu_0 + \delta\nu \\ \nu(\pi) &= \nu_0 \\ \nu(\sigma^-) &= \nu_0 - \delta\nu \end{aligned} \qquad (1)$$

where $\delta\nu$, the shift in the frequency due to the Zeeman effect, is given by

$$\delta\nu = (g_J\beta/h)H$$

where g_J is the Landé g factor, β is the Bohr magneton, h is Planck's constant, and H is the magnetic field strength.

The absorption profile of mercury in air is pressure-broadened (*2*) so that the absorption width is much wider than the Doppler width. However, $\delta\nu$ is linear in a magnetic field, H, so that, at least in principle, if the magnetic field is increased, two of the Zeeman components, σ^+ and σ^-, will lie outside the absorption profile, and the π component will lie inside the absorption profile. At atmospheric pressure, the Doppler effect is negligible, and the absorption broadening is entirely due to the pressure effect. On the other hand, the line profile of the resonance radiation is that of the Doppler width of the low-pressure electrodeless mercury lamp. We made this lamp with an effective lamp temperature of about 300°K. The shape of the 2537-Å light profile was checked with a Fabry-Perot interferometer as well as by Bitter's mangetooptical scanning method (*3*).

In order to determine the trace mercury from the host material with no initial chemical separation, we heated the host material in the absorption furnace to decompose its mercury compounds to mercury metal. In addition to mercury, complex chemical by-products also fill the furnace, whether we heat the host material in air or in an oxygen-rich atmosphere. These nonmercury components either scatter or absorb the 2537-Å radiation. This phenomenon has hitherto made the determination of trace mercury to even 10 ppm impossible without prior extraction of metallic mercury from the host material. However, the absorption or scattering by nonmercury vapors in general varies very slowly in the vicinity of 2537 Å, so we can assume that it is the same for the σ^+, π, and σ^- lines. Thus, if we construct a device that detects the difference of absorption between the total monitoring light $I_S = I(\sigma^+) + I(\sigma^-) + I(\pi)$ and the reference light $I_R = I(\sigma^+) + I(\sigma^-)$, we get the effect of absorption by mercury only, provided the absorption by nonmercury vapor is not close to 100 percent. Figure 1 is a block diagram of such a device. Because there is a mercury cell (Hg in 1 atm of Ar or N_2) in front of photodetector 2, the intensity I_R of the light impinging on this detector is entirely due to the σ^+ and σ^- components and is given by

$$I_R = I(\sigma^+) + I(\sigma^-) = I_{out}$$

whereas the intensity I_S of the light impinging on photodetector 1 contains all the components and is given by

$$I_S = I(\sigma^+) + I(\sigma^-) + I(\pi) = I_{out} + I_{in}$$

Here S refers to light containing the signal due to mercury, and R stands for the nonmercury reference; I_{out} refers to the intensity of the Zeeman components lying outside the absorption profile and I_{in} to the intensity of those lying within. The photoelectric current, and hence the output voltages

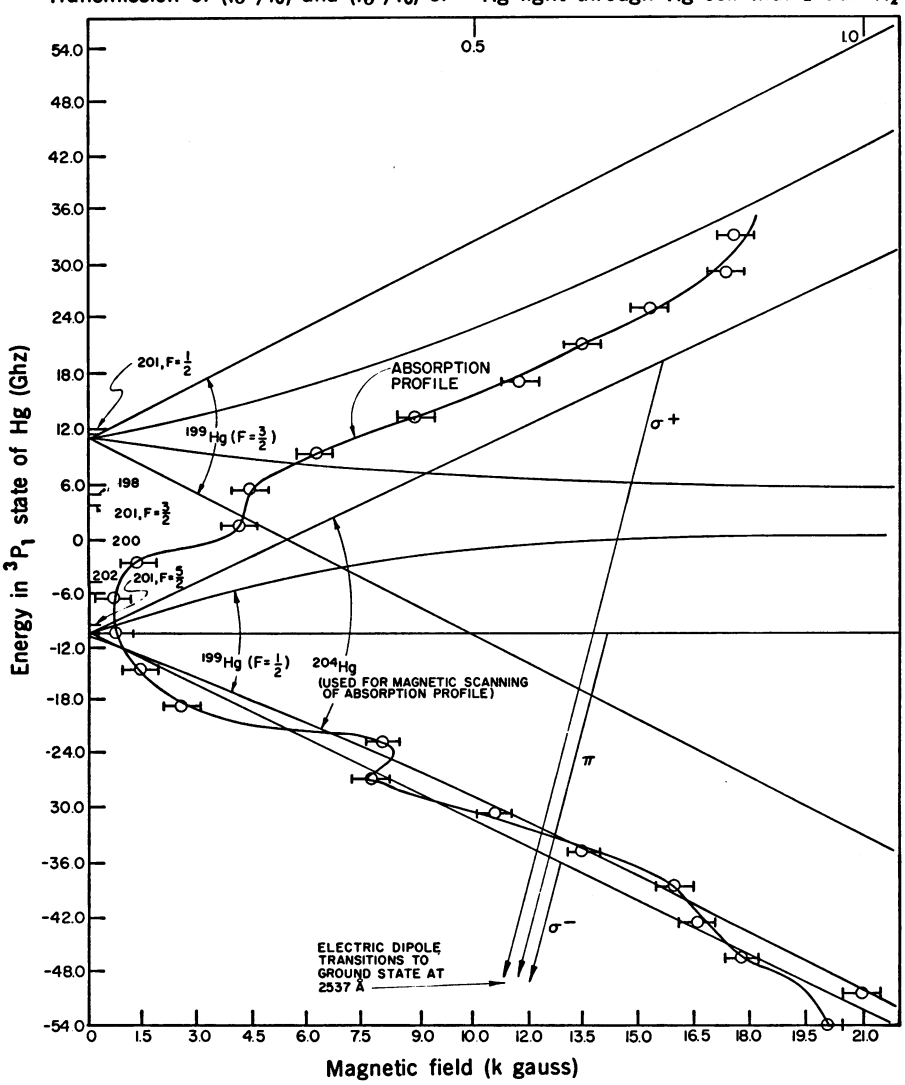

Fig. 2. Energy levels of the 6^3P_1 states of the natural mercury isotopes and the Zeeman pattern of ^{198}Hg and ^{204}Hg. Superimposed on the figure is the pressure-broadened shifted profile of the 6^3P_1 state of natural mercury experimentally traced by a magnetic scanning technique; Zeeman-shifted σ^+ and σ^- light of ^{204}Hg at wavelength 2537 Å was used. I/I_0 = (transmitted intensity)/(incident intensity).

of photomultipliers 1 and 2, is proportional to I_S and I_R. Thus, the output voltages can be represented as

$$V_S = k_1 I_S \text{ and } V_R = k_2 I_R$$

where k_1 and k_2 account for the quantum efficiency of the photodetectors, the gain, the geometrical factor, and so on. In the absence of a sample containing mercury in the absorption cell, we can set $V_{out} = V^0_{out} = V_S - V_R = 0$, by adjusting either the light intensity I_S and I_R or the amplifier gains A_1 and A_2 (see Fig. 1). Thus we have

$$V_{out} = V^0_{out} = k_1 I_S - k_2 I_R = 0 \quad (2)$$

so that

$$k_1 = \frac{k_2 I_R}{I_S} = \frac{k_2 I_{out}}{I_{out} + I_{in}} \quad (3)$$

If we now introduce a sample of the host material containing mercury into the absorption cell (furnace), the transmitted light intensities I_S and I_R are given by

$$I_S = I_{in}(1 - \alpha_{Hg} - \alpha_n) + I_{out}(1 - \alpha_n)$$
$$I_R = I_{out}(1 - \alpha_n) \quad (4)$$

where α_{Hg} is absorption by mercury and α_n is absorption or scattering by nonmercury elements or smoke. Therefore

$$V_{out} = k_1 I_S - k_2 I_R = -k_1 I_{in} \alpha_{Hg}$$
$$= -k_2 \left(\frac{I_{out}}{I_{in} + I_{out}} \right) I_{in} \alpha_{Hg} \quad (5)$$

Thus, V_{out} is proportional to the mercury absorption, and the effect of nonmercury is completely eliminated.

In the actual practice of detecting mercury in the host material, it is not convenient to use the normal Zeeman effect described above; the width of the absorption profile is so large, because of pressure broadening, that we would need an unreasonably large (more than 20 kgauss) magnetic field to obtain I_{out} sufficiently far away from the absorption profile. This would add the cost and weight of a relatively large magnet to the instrument. To overcome this difficulty, we used a ^{199}Hg source, since the hyperfine structures of ^{199}Hg in the $^3P_1$ state lie at the extreme ends of the isotope distribution of natural mercury.

Figure 2 shows the Zeeman effect of ^{199}Hg along with the energy levels of the natural mercury isotopes. From Fig. 2 it is evident that we gain about 12 Ghz in Zeeman separation over the normal Zeeman effect we discussed previously [$^{199}\Delta\nu(^3P_1) = 22{,}128.650$ Mhz] (*4*). However, the pressure-broadened profile of natural Hg (about 10 percent ^{198}Hg, 28 percent ^{200}Hg, 13 percent ^{201}Hg, and 20 percent ^{202}Hg) overlaps these two hyperfine levels in a zero magnetic field, so we need a further shift in the hyperfine lines. This can be accomplished by the Zeeman effect.

A magnetic field of about 10 kgauss can shift the hyperfine Zeeman levels $|F = 3/2,\ m_F = 3/2\rangle$; $|F = 3/2,\ m_F = 1/2\rangle$; and $|F = 1/2,\ m_F = -1/2\rangle$ of ^{199}Hg sufficiently far away that the optical Zeeman components originating from these three levels can be used as I_{out}, described earlier. The remaining Zeeman lines, originating from $|F = 3/2,\ m_F = -1/2\rangle$; $|F = 3/2,\ m_F = -3/2\rangle$; and $|F = 1/2,\ m_F = 1/2\rangle$, play the role of I_{in}. Thus we were able to use a light-weight permanent magnet and still obtain sufficient shifts in the hyperfine structure Zeeman lines to obtain an I_{out} reference signal for elimination of the nonmercury effect.

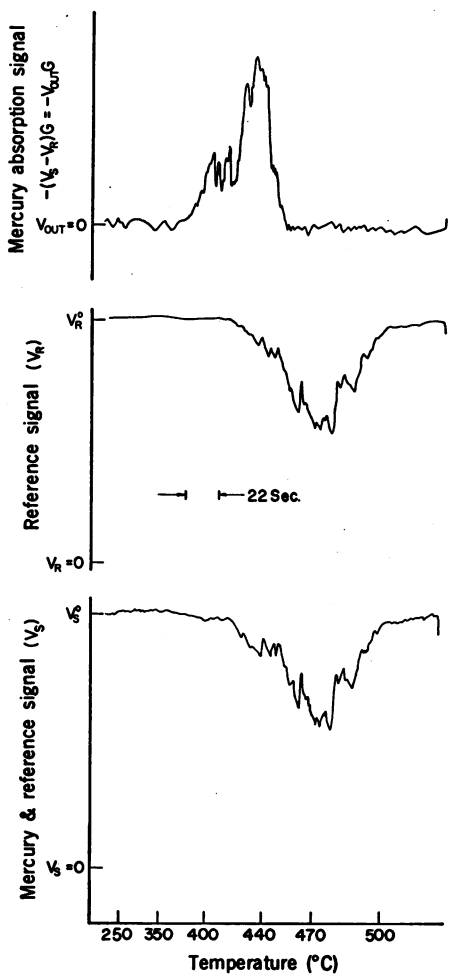

Fig. 3. Recorder tracings of V_S, V_R, and amplified Hg signal, $(-G)(V_{out})$, for tuna meat, where $-G$ is the gain of the amplifier with integration time constant 0.1 second. The large drop in V_S and V_R is due to the smoke effect. The temperature indicated is the temperature of the furnace; the temperature of the sample is lower by about 50° to 100°C.

The performance of the instrument was tested against a standard, made by mixing HgI into carbon and HgO into carbon and starch. In addition, we ignited various materials containing no mercury to ascertain that V_{out} remained zero in the absence of mercury, in spite of smoke, steam, and so forth. We also used our standard to determine k_1 and k_2 and to calibrate the instrument. The apparatus was used to test for mercury on tuna supplied and analyzed (by standard chemical analysis) by the National Canners Association; we obtained good agreement with our standard. We placed varying amounts of tuna containing 0.49 and 0.24 ppm of Hg in the furnace and plotted the number of nanograms of Hg against the area under the Hg absorption signal. All samples were within 12 percent of the average over the range 5 to 35 ng. After these tests, we measured mercury concentrations in various materials such as wall paints, papers, and meats. Figure 3 shows a typical signal V_{out} along with V_R and V_S.

This technique is not limited to the detection of mercury; we believe it can be extended to almost every element for which the atomic absorption technique is applicable. The block diagram (Fig. 1) illustrates only the principle behind the instrument. In the actual instrument we used an automatic heating furnace, a phase-sensitive detector to eliminate extraneous light interference, and a digital integrator. The performance of the instrument would be improved by the use of an automatic light-intensity stabilizer and an automatic gain control against the attenuation of I_R and I_S due to α_n.

Barringer (*5*) and, independently, Ling (*6*) obtained I_R from the wing of the pressure-broadened 2537-Å emission line to monitor the nonmercury effect. The basic difference between Barringer's and our instrument is that we used a sharp spectral line of 5.5 gauss Hg (FWHM) while, from Fig. 2, Barringer's spectral line must be at least 48 gauss Hg (FWHM). Since $\Delta\nu$ (lamp)/$\Delta\nu$ (absorption) is about 1/9 in our instrument, the variation in $\Delta\nu$ (lamp) due to temperature and to power variation in the light source causes no serious error in Hg determination. Ling used pressure-broadened

resonance fluorescence for I_R. We believe that the intensity of the resonance fluorescence would be quite weak.

No great effort was made to increase the capability of our instrument to the limit. With improved electronics it should be possible to determine Hg as low as 10^{-11} g/cm^3, corresponding to a sensitivity of about 1 ppb for a 10-mg sample.

T. HADEISHI
R. D. MCLAUGHLIN
Lawrence Radiation Laboratory, University of California, Berkeley 94720

References and Notes

1. B. Cagnac, *Ann. Phys.* **6**, 467 (1961).
2. See, for example, A. C. G. Mitchell and M. W. Zemansky, *Resonance Radiation and Excited Atoms* (Cambridge Univ. Press, New York, 1962).
3. F. Bitter, H. Plotkin, B. Richter, A. Teriotdale, J. E. R. Young, *Phys. Rev.* **91**, 421 (1953).
4. F. Bitter, *Appl. Opt.* **1**, 1 (1962).
5. A. R. Barringer, *Inst. Mining Met. Bull. No. 714* **75B**, 8120 (1966).
6. C. Ling, *Anal. Chem.* **39**, 798 (1967); *Anal. Chem.* **40**, 1876 (1968).
7. We thank M. Nakamura for assistance and advice regarding electronics, M. Michel for discussion of the chemical processes that may take place in the furnace, W. Berlund for glass-blowing, and D. Escobales for furnace design. This work was done under the auspices of the Atomic Energy Commission.

17 June 1971; revised 5 August 1971

Riboflavin Photosensitized Oxidation of 2,4-Dichlorophenol: Assessment of Possible Chlorinated Dioxin Formation

Abstract. *Dimeric products are formed by riboflavin-sensitized photooxidation of 2,4-dichlorophenol. The products of this reaction were examined to determine whether chlorinated dibenzo-*p*-dioxins could be formed from chlorophenols in water by the action of light of wavelengths greater than 280 nanometers. Dimers are formed by union of phenoxy radicals through carbon-carbon or carbon-oxygen bonds. 4,6-Dichloro-2-(2,4-dichlorophenoxy)phenol was obtained in greater quantity than other dimers. Products were characterized by combined gas chromatography and mass spectrometry. Chlorinated dibenzo-*p*-dioxins which could result from ring closure of a 2-phenoxyphenol derivative were not detected in the products of photolysis. The failure to detect chlorinated dibenzo-*p*-dioxins may result from the rapid photolytic breakdown of the lower chlorinated dibenzo-*p*-dioxins. Under environmental conditions, dioxins are unlikely products of the lower chlorinated phenols or phenoxyalkanoic acids.*

Chlorinated dibenzo-*p*-dioxins are formed by pyrolysis of chlorophenols and their salts (*1*). The extremely high mammalian toxicity and teratogenic potential of the chlorinated dioxins are significant because of their possible occurrence as contaminants of commercial chlorophenols and their derivatives (*1*, *2*). A report that riboflavin sensitized the photodecomposition of 2,4-dichlorophenoxyacetic acid (*3*) prompted us to investigate the course of riboflavin-sensitized photooxidation of 2,4-dichlorophenol and especially the possibility that sensitized photolysis of 2,4-dichlorophenol may give a chlorinated dioxin by dimerization and loss of hydrochloric acid. Although Joschek and Miller did not detect dibenzo-*p*-dioxin during irradiation of phenol, carbon-carbon and carbon-oxygen dimers were formed (*4*). In the presence of photoexcited dyes similar reactions may occur through intermediate phenoxy radicals (*5*). Other photochemical reactions of chlorophenols have been reported. Under mercury arc irradiation in organic solvents, chlorinated phenols are reductively dehalogenated (*6*), and, in water, replacement of halogen by hydroxyl is possible (*7*).

Sunlight irradiation of the rice herbicide, pentachlorophenol, gives a number of products. Munakata and Kuwahara elucidated the structures of these and found that some dimeric ethers were formed (*8*). Later work indicates

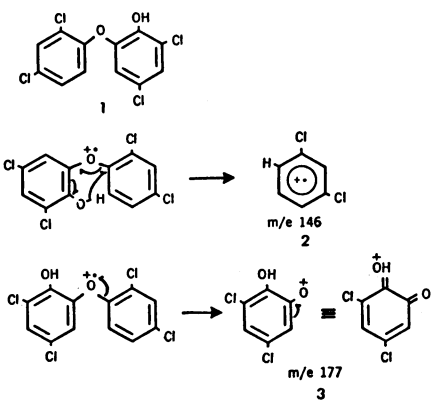

Fig. 1. Mass spectroscopic fragmentation of **1** to produce ions **2** and **3**.

that octachlorodibenzo-*p*-dioxin can be formed by photolysis of pentachlorophenol (*9*).

The herbicides 2,4-D (2,4-dichlorophenoxyacetic acid) and 2,4,5-T (2,4,5-trichlorophenoxyacetic acid) are manufactured by condensation of the corresponding phenol with sodium chloroacetate. Since the photolysis of these herbicides in water yields chlorophenols (*7*), it is important to establish the ultimate fate of chlorophenols in the environment.

We have now demonstrated that photosensitized reactions of 2,4-dichlorophenol irradiated in water (at a wavelength greater than 280 nm) yields principally dimeric products. Only trace quantities of dechlorinated products could be detected.

A saturated solution of 2,4-dichlorophenol in water saturated also with riboflavin was irradiated at room temperature by a 450-watt mercury lamp with a borosilicate glass filter for 1 hour to obtain maximum yield of dimer. Oxygen was bubbled through the solution and, since yields were much lower in the presence of nitrogen, we concluded that oxygen may function in regenerating riboflavin from its photoreduction product (*10*). Products were isolated and examined by combined vapor phase chromatography and mass spectrometry (*11*).

Mass spectrometry of the products and their methylated derivatives showed that tetrachlorinated phenoxyphenols and tetrachlorodihydroxybiphenyls were present. A trace quantity of a trichlorophenoxyphenol was also obtained. There was no evidence of ring closure to a substituted dibenzo-*p*-dioxin.

The tetrachlorophenoxyphenols were shown to be a mixture of two isomers separated by thin-layer chromatography on silica gel GF_{254} in benzene (Fig. 1). The major product was allocated structure (**1**), 4,6-dichloro-2-(2,4-dichlorophenoxy)phenol. The mass spectrum showed molecular ion at *m/e* (mass/charge) 322; and ratios of abundances of peaks at *m/e* 322, 324, 326, and so on confirmed the presence of four chlorine atoms in the molecule. A peak at *m/e* 146 (two Cl atoms) (**2**) is indicative of an *o*-phenoxyphenol, since the hydrogen transfer shown is typical of the fragmentation of an orthohydroxyphenoxy ether (*12*). A fragment, *m/e* 177 (two Cl) (**3**), indicates the presence of the phenoxyphenol system, as does also the formation of a monomethyl ether, *m/e* 336, on treatment